SEMI-AUTOMATED TECHNIQUES TO MEASURE ULTRASONIC PROPAGATION PROPERTIES USING A SCANNING LASER ACOUSTIC MICROSCOPE

BY

ANDREA MARIE MRAVCA

B.S., University of Illinois, 1980

THESIS

Submitted in partial fulfillment of the requirements
for the degree of Master of Science in Electrical Engineering
in the Graduate College of the
University of Illinois at Urbana-Champaign, 1981

Urbana, Illinois

ACKNOWLEDGEMENTS

There are many people to whom I am deeply indebted for their assistance, cooperation and patience in the evolution of this manuscript. Sincere gratitude is extended to Professor W.D. O'Brien, thesis advisor and friend, who suggested the topic for this study and offered unending aid and advice throughout. Much appreciation also goes to Dr. John Erdman and Mary Grummer (Department of Food Science) with whom I collaborated in obtaining the necessary biological specimens and other pertinent data.

I am very grateful to Steve Foster, whose Data Acquisition System I incorporated into my project, who devoted an extensive amount of time to writing the required programs and discussing the countless technical difficulties. Genuine appreciation also goes to Dave Dubeck and Dr. Ron Johnston for their continued technical support. In addition, much thanks is dedicated to Bob Cicone for the drawings, Mrs. Wanda Elliott and Mike Haney for their advice in the preparation of this paper, and Charlie Edwards for his helpful suggestions and friendship.

Special notes of thanks to those who, across the miles, persevered with me: my loving family who bestowed upon me their confidence, support and encouragement, and Paul Davoust, my very dear friend, who made the last six months priceless.

TABLE OF CONTENTS

CHAPTER 1

INTRODUCTION

The Scanning Laser Acoustic Microscope (SLAM) is an advanced ultrasonic instrument for examining the elastic properties of materials and biological media at the microscopic level. It employs a combination of a laser beam probe and ultrasonic waves to detect variations in the microstructure of the specimen under examination. Sound waves are generated from a transducer mounted in the bottom of a fused quartz block and oscillate at a frequency of 100 MHz. The sound impinges on the sample located on the top of the block, or the stage. From above the sample, the transmitted sound is detected by the scanning laser beam. The reflected light from the beam becomes modulated by the sonic energy at every point on the field of view. The image of the sonic field, termed an acoustic micrograph, is then displayed on a T.V. monitor.

Acoustic microscopy, using the SLAM, is an advantageous technique enabling high resolution (1-20 μm) in the characterization of tissue. The Bioacoustics Research Laboratory at the University of Illinois (Champaign-Urbana) has employed a SLAM in extensive studies of a variety of tissue in order to quantize acoustic attenuation and velocity of the specimens. Investigations of the past and the implications for the future were the two sources of motivation for this thesis.

The measurement techniques of previous investigations were completely manual and somewhat subjective. Additionally, the

human error varied from one operator to another. For these reasons, a system to measure acoustic tissue parameters was needed which would semi-automate, as well as improve the precision of, the measurement techniques. The primary purpose of this study was, thus, defined by this need.

A secondary purpose, in order that the techniques be verified, was to actually collect some data. It was decided to work with liver tissue because it is one of only a few homogeneous biological organs. Furthermore, since extensive data had already been collected for "normal" livers, it was suggested that "fatty" livers be included in this study. Since there is no preferential localization of the fat in any portion of the liver, a "fatty" liver is also a homogeneous medium (Lieber et al., 1965). A decision to measure the attenuation and velocity of livers ranging in fat content (including "normal"), was made in hopes of seeing a correlation between the tissue parameters and the percentage fat. The implications of such a relationship could prove to be extremely beneficial in the future for clinical medicine. Fatty liver disease, either from high alcohol consumption, or protein deficient diets, is very common in today's society. Early detection of this seriously damaging disease by a non-destructive technique could open up many new areas of interest for the world of acoustic microscopy.

CHAPTER 2

MEASUREMENT TECHNIQUES

2.1 VELOCITY

The Scanning Laser Acoustic Microscope, SLAM, operating in the interferometric mode, has been employed in the quantitative determination of velocity of a variety of materials. In this mode, changes in the acoustic phase are measured as the wave propagates from the microscope stage to the coverslip through the material under investigation. This is accomplished within the SLAM by the electronic mixing of the video signal from the detector and a reference frequency. Conceptually, this can be thought of as the intersection of two plane sound beams at the coverslip, both having the same frequency, and producing a stationary ripple pattern which results in a series of regularly spaced, vertical fringed lines being displayed on a T.V. monitor. The angle between the two beams, which determines the spacing of the fringed lines on the screen, changes if traveling from one medium to another whose velocity sound characteristics differ. For example, an object whose sound velocity is greater than that of the surrounding medium would interrupt one of the beams causing localized, lateral shifts of the fringes to the right. Figure 1 illustrates an interference pattern of a single collagen thread in a saline solution. The displacement of a fringe is dependent on the thickness of the object and is related to the difference in transmission times of one sound beam compared with the unperturbed beam.

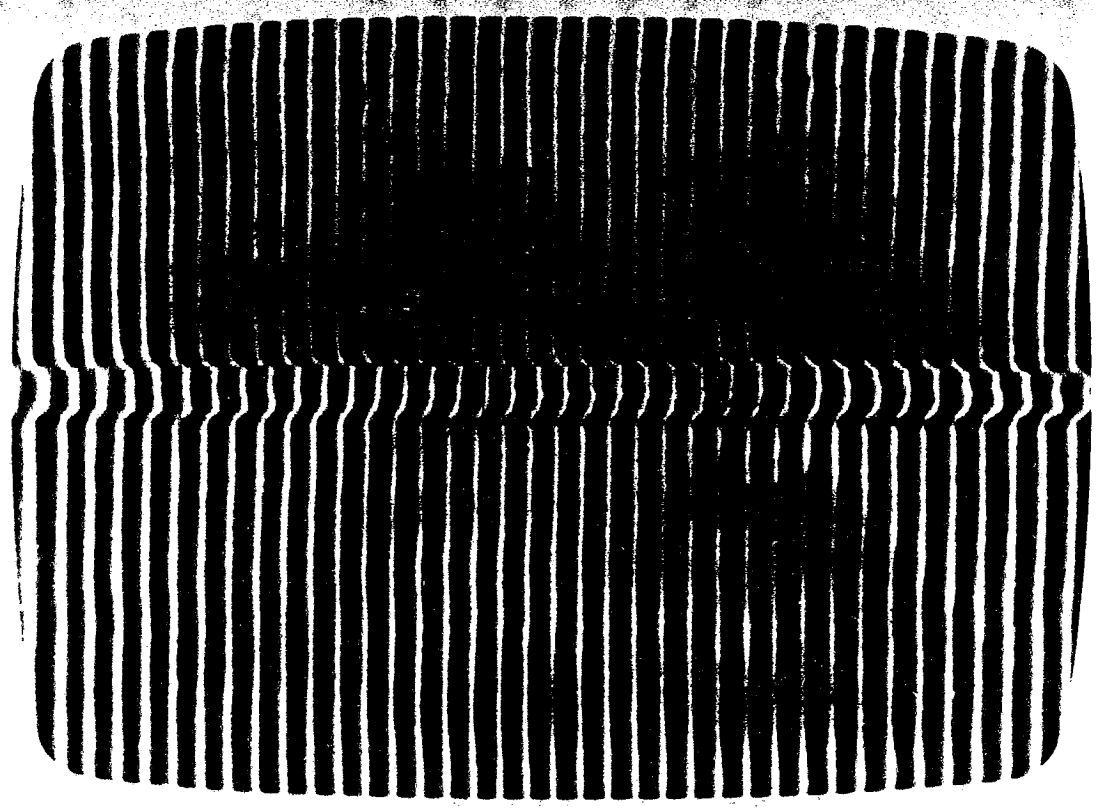

Figure 1 Interferogram of a collagen thread in a saline solution.

The velocity of sound through an object can be calculated using a formula derived in an unpublished paper by L.W. Kessler and P.R. Palermo (Sonoscan,Inc., Bensenville, Illinois). The development and subsequent results can also be found in a published paper by Goss and O'Brien (1979). The equation for the ultrasonic velocity in a specimen is given by

$$Cx = \frac{Co}{\sin\theta o} \sin\left[\tan^{-1}\left(\frac{1}{(1/\tan\theta o) - (N\lambda o/\tan\theta o)}\right)\right] \qquad (1)$$

where Co is the velocity of sound in the surrounding medium, θo is the angle of the beam from the normal in the surrounding medium, λo is the wavelength of the sound in the surrounding medium, and N is the normalized lateral fringe shift, or the ratio of the distance of the lateral shift of the known fringe to the unknown fringe (ad) to the distance between two adjacent known fringes (ab).

To find θo Snell's law is used

$$\theta o = \sin^{-1}\left[\frac{Co}{Cs} \sin\theta s\right] \qquad (2)$$

where Cs is the velocity of sound in the fused silica of the microscope stage (Cs = 5968 m/s) and θs is the angle of the sound beam with respect to the normal in the fused silica stage ($\theta s = 45^{o}$).

When the "unknown" specimen is biological tissue, saline is usually used as the surrounding medium because it is isotonic with the liver, i.e., the saline will not be absorbed by the tissue to

cause a size increase, nor will it extract the natural fluids from the tissue to cause a decrease in size. For saline, Co = 1520 m/s and $\theta o = 10.4^{o}$.

The previous technique which was to be improved upon required photographing the interferograms off of the T.V. monitor, having them processed into slides, and then enlarging them into 5" x 7" photographs. The parameters, ab and ad, could then be measured from the prints and the normalized fringe shift, N, calculated. Assuming uniformity in the thickness of the tissue, any area of the image was chosen at which to work if the nonperturbed interference lines were clearly seen both above and below the lateral shift. Vertical lines were drawn to connect the unperturbed fringed portions of two adjacent lines, and the distance between these two lines was measured and recorded as length ab as illustrated in Figure 2. Another vertical line was then drawn through the laterally shifted line and parallel to the other two lines. The distance between this line and that drawn through the unshifted interference line was ad and was also measured and recorded.

Using this method, the photographed interference lines were difficult to resolve because the photographs were thick and indistinct, as seen in Figure 2. Ideally, the fringed lines portrayed on the T.V. monitor should be one point wide, with the center, or maximum, being detected for each interference line on each raster line. However, the full dynamic range of the microscope is larger than the dynamic range of the detection scheme, resulting in the detection of other points which lie

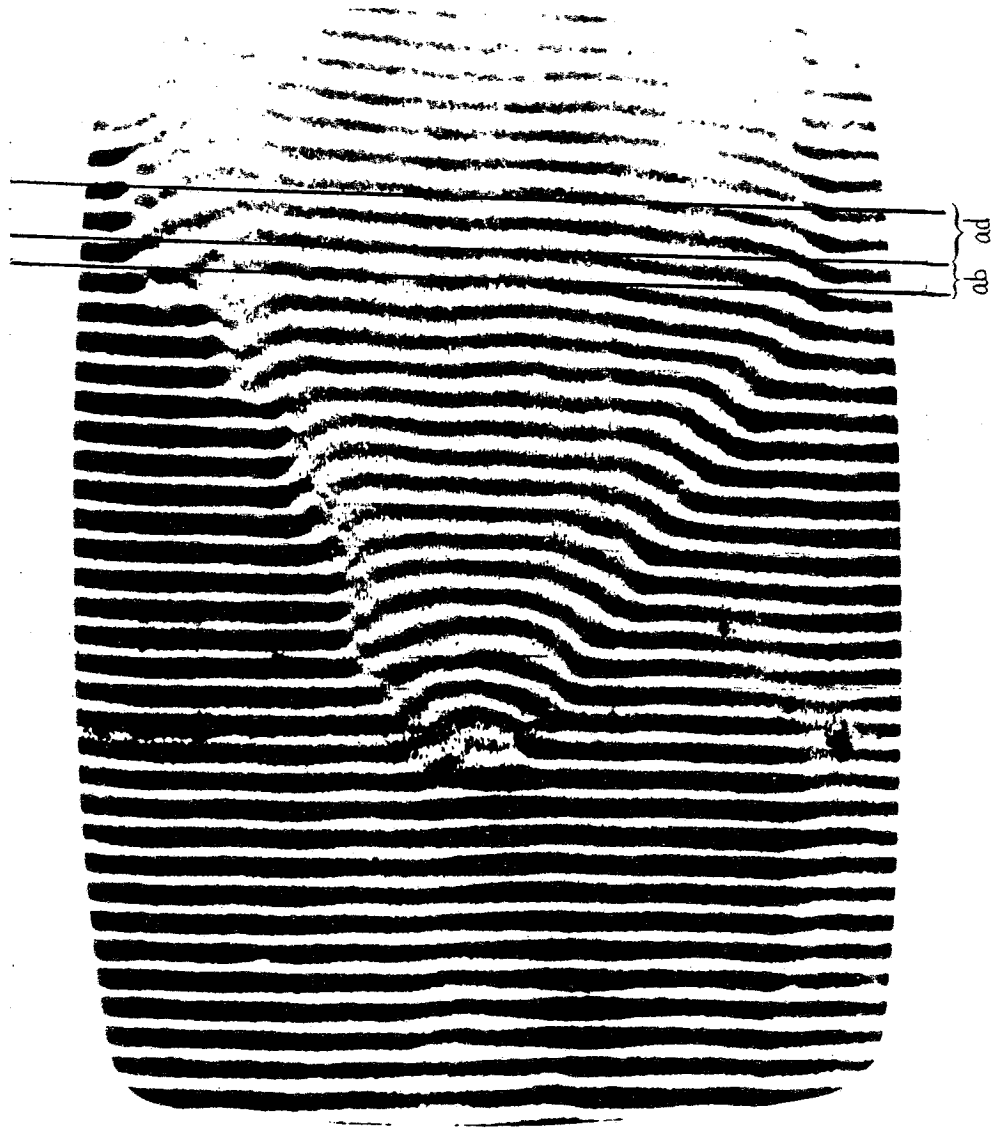

Figure 2 Determination of N.

within a certain range of the center point. This results in the "band" of points for each interference line, as portrayed on the T.V. monitor. If it was known that the process was linear, i.e., that an equal number of points were detected on both sides of the center point, the center of each interference line could be found by dividing each "band" of points down the middle. However, the status concerning the linearity of the process was unknown, so there was always some question concerning the actual placement of the lines to be drawn for the ab-ad measurements; therefore, a new technique of producing the interference lines was necessary. Also desired was a faster, easier system to accrue permanent copies of each interference pattern.

The technique undertaken to solve this problem was prompted by work being done to digitize the image from the acoustic microscope in the Bioacoustics Research Laboratory (Foster, 1981). The results of his research were able to be used directly in this experimentation. A brief description of the system is given below; for further details see Foster (1981).

A data acquisition system (DAS) to interface between the SLAM and a 32-bit mini-computer (Perkin-Elmer Model 7/32) was designed and built in order to digitize, store and manipulate images from the SLAM. Two separate pieces of equipment make up the DAS; an rf amplifier which is local to the SLAM, and a digitizer which is local to the computer. The amplifier takes a single line of the image off the SLAM monitor and transmits it to the receiving end of the digitizer where it is changed to binary code by an 8-bit, 30 MHz analog-to-digital (A/D) converter and then temporarily

transfered to a high-speed buffer memory (also part of the digitizer hardware). The buffer (1024 x 16 bits, 35 ns access time) then transmits its contents into computer memory after a complete line of a television frame has been digitized. This last step occurs at approximately 50 kHz.

The DAS utilizes the voltages of the video signal as the means of conversion to a digital signal which are then stored. The input range of the A/D is 1.0 V, so the signal of the image being digitized must be monitored to remain between -500 mV and +500 mV. Since the format to the processor is an 8-bit output, the largest decimal number able to be stored is 255. In accordance with the existing hardware, a digital voltage of 255 represents -500 mV, the brightest possible image and largest signal; the digital voltage decreases with decreasing signal strength.

Two programs from the DAS project, described in detail in Foster (1981), were incorporated into a useful, semi-automated system to achieve hard copies of the interferograms. The first program digitizes the entire image, stores it on tape, and then averages it n number of times, where n is chosen by the operator and has a range from 1 to 64, inclusive. Improved noise performance is accomplished by employing a complicated running average approach in order to average out a slight horizontal drift of the SLAM, however, the time for completion increases as n is increased. The effects of varying n are illustrated by means of examples in Foster (1981). For this work it was decided to average each image 16 times.

The second program enhances the interference lines taken from the SLAM by using a correlated receiver. An ideal cross section of an interference line that has been stored in memory is compared with the raster line waveform and an interference line is detected when a relative maximum occurs in the correlated result. The width of the filter of the correlated receiver is chosen by the operator from the range of 1 to 16 data points, inclusive. An increase in the number of data points of the filter offers better resolution (Foster, 1981), but also takes a longer time for completion. A filter width of 8 data points was used in this work for the velocity measurements; a compromise between time and precision. The detected interference line points are stored until all 482 lines of the image have been correlated. A hard copy of the enhanced interferogram is then printed out in two sizes; a condensed one comparable in size to the image on the T.V. monitor, and a larger one true in size to the resolution of the digitizer.

The improvement using this technique is a result of the electronic detection of the center of each fringe line by the correlated receiver. The computer printout, thus, consists of interference lines that are the width of a single data point. The enhancement in the hard copy of an interference pattern can be seen by comparing the photograph of Figure 3 to the digitization of Figure 4.

The larger of the two image replications is then used for the fringe shift determination. Manual techniques are still necessary for the task of determining the ab-ad measurements. The improvements here are that there is a much larger working area and

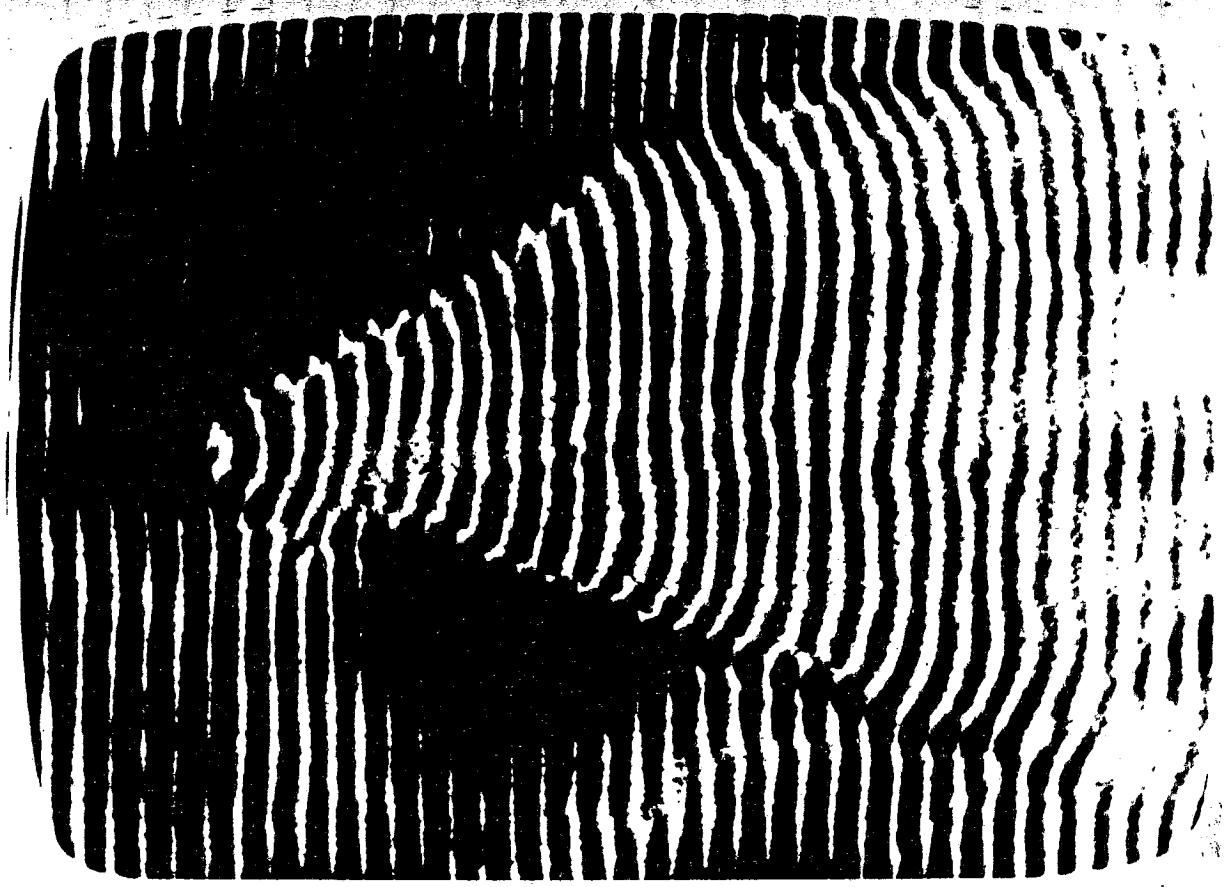

Figure 3 Photograph of an interferogram.

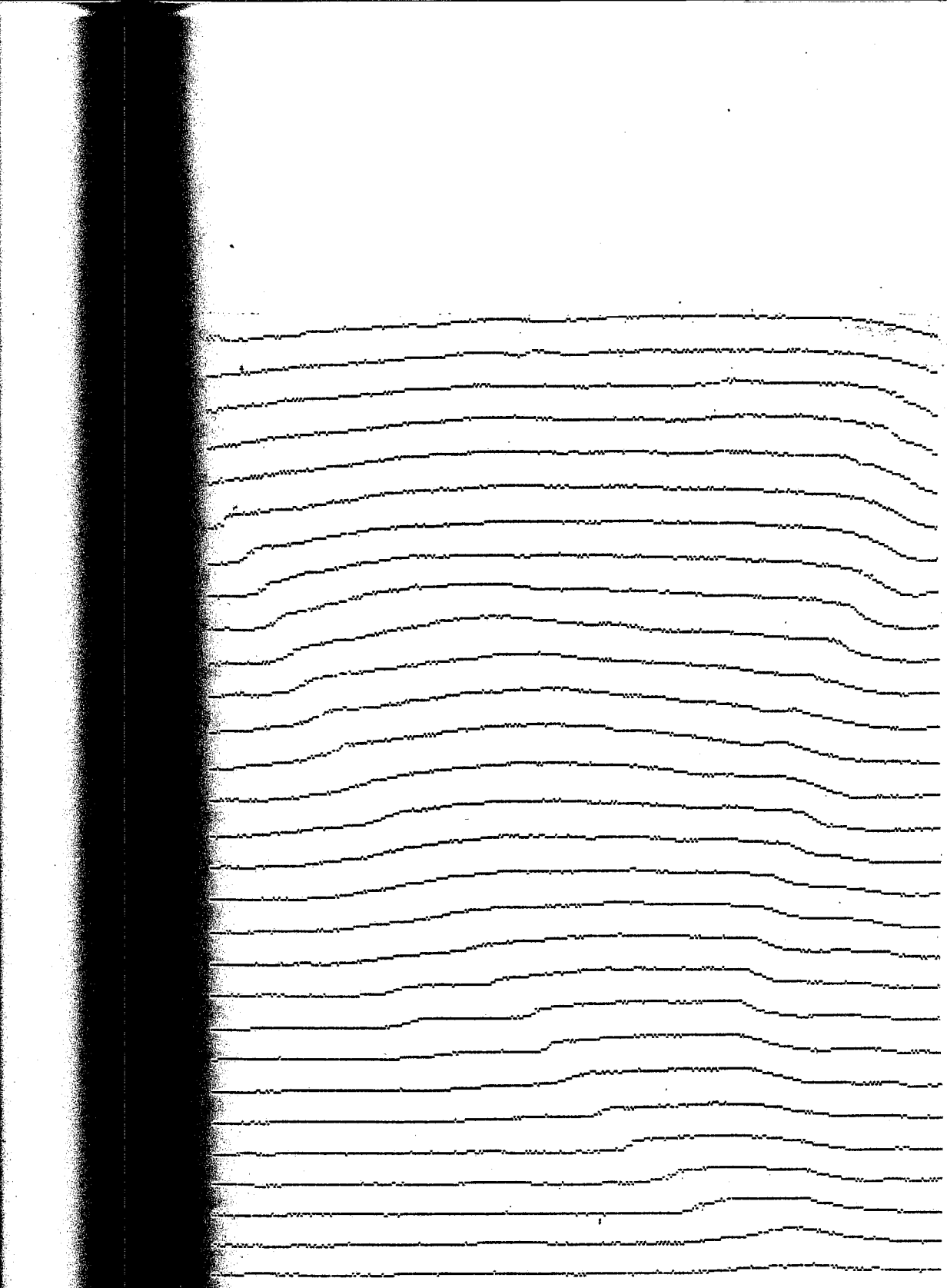

Figure 4 Digitization of the same image in Figure 3.

there is an increased resolution of the interference lines. As a result, there is increased precision and accuracy of N.

When working with tissue slices from the same specimen, a change in the thickness will yield a subsequent change in N. The ratio of N to T, howvever, should remain constant. To assure a consistency in the ratios, it was decided to work with four different thicknesses from each liver sample. The thicknesses were chosen so that they could easily be cut using the microtome, a device used for cutting very thin sections of frozen tissue, and, also, so that they could be used for the attenuation measurements. The thicknesses are 360 μm, 540 μm, 720 μm, and 900 μm.

To obtain a range of Cx (Equation 1) values it is necessary to work with all thicknesses of a sample. The two unknown parameters, N and T, both contain some degree of error or uncertainty, so the maximum and minimum of these two values must be found for the Cx range determination. It can be seen from Equation 1 that the largest N with the smallest T results in a maximum Cx, while the smallest N and largest T results in a minimum Cx.

Quantification of the range of N values for each thickness is made by obtaining several ab-ad measurements, calculating N, and taking only the highest and the lowest values. This must be done for each specimen looked at under the microscope, as the range of each liver sample may vary.

The error of T is inherent in setting the desired thickness on the microtome and bringing the tissue down over the knife edge

and, therefore, is independent of the thickness being sliced. To quantize the error, ten tissue slices were cut at a prescribed thickness, 360 μm, and immediately measured to an accuracy of 0.01 mm using a Starrett Metric Micrometer Caliper. The standard deviation was calculated to be 49 μm, and this value then used to assess the maximum and minimum thicknesses of each sample, namely, 360 ± 49 μm, 540 ± 49 μm, 720 ± 49 μm, and 900 ± 49 μm. The maximum values, T(max), are 409 μm, 589 μm, 769 μm, and 949 μm. The minimum values, T(min), are 311 μm, 491 μm, 671 μm, and 851 μm.

Once the extreme values of N and T are found at each thickness the ratios of N(max) to T(min) and N(min) to T(max) are formed, and the respective Cx(max) and Cx(min) values are calculated. For each liver sample only the largest Cx(max) and smallest Cx(min) are chosen, thus, establishing a range of sound velocity measurements for each sample. An average velocity can be calculated by finding the mean of Cx(max) and Cx(min) if it is known that the velocity values are uniformly distributed within the determined range of Cx.

2.2 ATTENUATION COEFFICIENT

Ultrasonic attenuation is the decrease in energy of the sound field as it propagates through a material. Many factors account for attenuation, including absorption and scattering. Absorption is the loss of energy due to heat transfer within the sample; scattering, which includes diffraction and reflection, is a redirection of the energy due to inhomogeneities of the sample.

There are several ways of making attenuation measurements; only one, the insertion loss method, was used in this investigation and will be described.

The insertion loss method involves the comparison of the received signal amplitude with and without a sample of a known thickness in the sound path. Insertion loss (IL) is usually measured in terms of decibels (dB) or nepers (Np) where 1 Np = 8.686 dB. The attenuation coefficient of a given material is a measure of the IL per unit thickness and is usually described in terms of dB/cm or Np/cm. This quantity is found by plotting IL versus sample thickness as shown in Figure 5. The slope of the line is the attenuation coefficient and the y-intercept is the IL due to the reflective losses at the interfaces.

The image portrayed on the T.V. monitor while the SLAM is in the acoustic mode is a measure of the relative transmitted acoustic energy where light areas correspond to high transmission (lower ultrasonic attenuation) and dark areas to low transmission (higher ultrasonic attenuation). To this end a comparison between the image brightness level with and without the specimen in the region of interest is a measure of the IL if the system is linear. Since the system is known to be nonlinear, IL measurements were formerly made on the SLAM in the interference mode using a subjective technique, which did not require the detection electronics to be linear, called the "Extinction" method.

In this previous procedure the operator would view on the T.V. monitor the image without the tissue on the microscope stage, choose a small area of the screen on which to concentrate and then

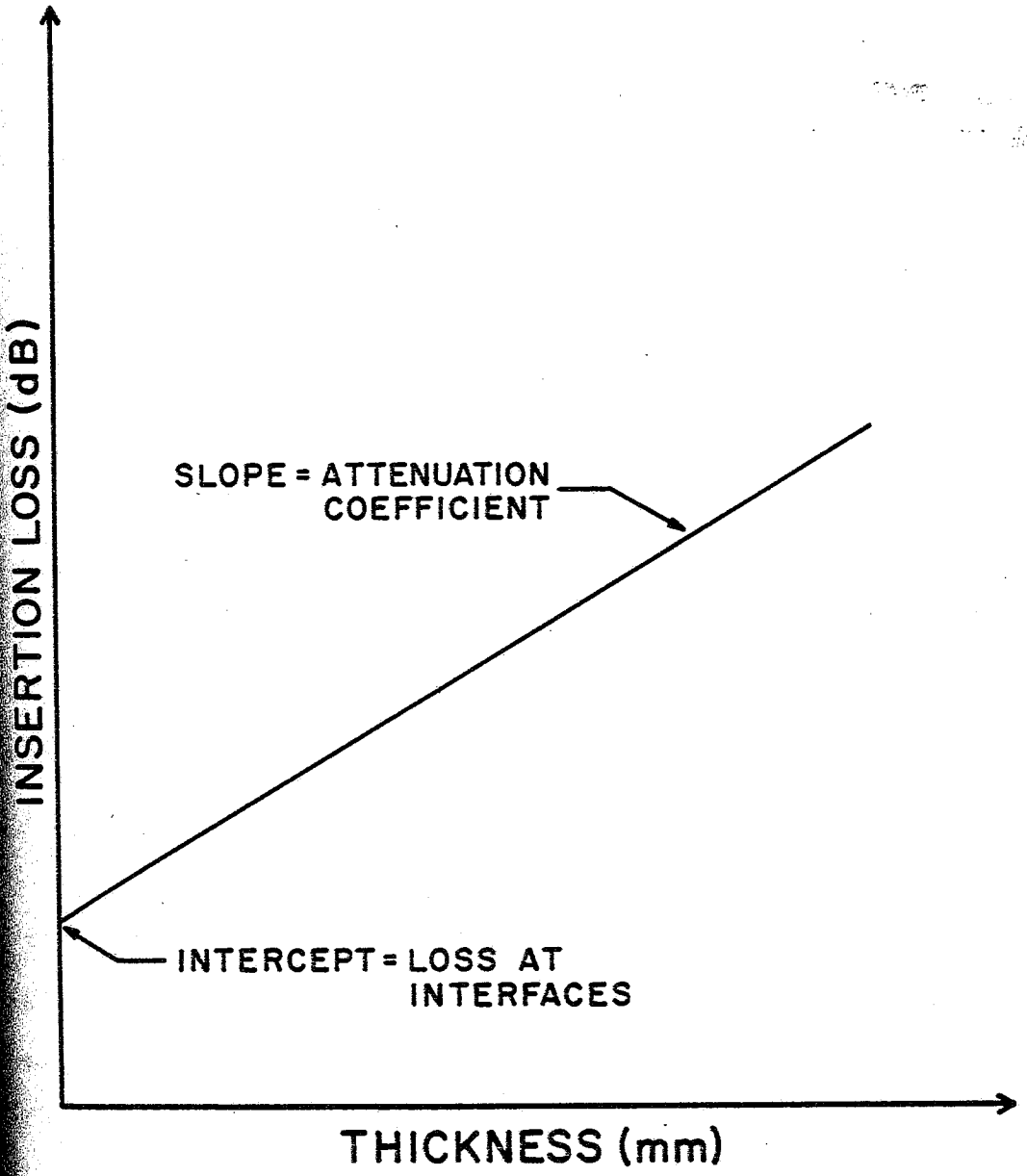

Figure 5 An example of an attenuation coefficient determination.

insert electrical attenuation between the oscillator and the transducer until the interference lines just disappeared. There was a certain degree of judgement as to when the interference lines were indistinguishable from the background noise of the image. Generally, the uncertainty in the electrical attenuation was about $\pm$ 2 dB (Pohlhammer et al., 1981). The tissue was then inserted into the field of view and, again, electrical attenuation was adjusted until the interference lines just disappeared. The difference in the two inserted attenuations is the acoustic loss provided by the specimen. The uncertainty of the IL values are, thus, twice that of the uncertainty of the inserted electrical attenuation values, or $\pm$ 4 dB. Subjectiveness on the part of the operator using this technique suggested the need for a semi-automated system. It was hoped in taking on this project that the precision of the new system would be improved over the $\pm$ 4 dB of the former technique.

The technique developed is compatible with the system for velocity measurements in that it makes use of the DAS which was already available. The reason behind employing the DAS is that IL can be found by using the stored digitized voltages and the following equation

$$IL = 20*\log\left(\frac{Vs}{Vo}\right) \qquad (3)$$

where Vs is the signal voltage and Vo is the reference voltage. The problems encountered in developing this technique and their subsequent solutions will be described.

The sound field is nonuniform which is clearly seen by the operator when the SLAM is in the acoustic mode. This is illustrated in Figure 6 where each number represents the average digital voltage in that area. Because of this unevenness it was necessary to choose an area of the image for voltage calculations and to select an optimal size of the area over which the average voltage remained constant. A valid IL of a sample could then be found by obtaining the average digital voltage of the selected area of the image both with and without the tissue.

Initially, the image was subdivided into a 16 x 16 array (containing 256 elements), at which the average voltage for each element was calculated and printed out. Since there are 482 raster lines of information and each raster line consists of 1536 points (30 MHz A/D converter), each array element consisted of 2880 data points (30 lines by 96 points). The first and last raster lines are omitted from the averaging for simplification, i.e., 16 divides 480 evenly. A program performed the averaging and printed out the array. An image of pure saline was digitized and voltage averaged at two different times (see Figures 6 and 7), and it was determined by comparing the pairs of digital voltages in the two output arrays, that there was a discrepency in the two arrays, i.e., some of the pairs of voltages differed by as much as 7. To quantify the discrepency, the deviation of D = 2.240 between the two arrays was calculated using the following equation

$$D = \left[\frac{1}{N} * \sum_{i=1}^{N} d_i^2 \right] **0.5 \qquad (4)$$

93	97	100	107	110	129	138	142	137	144	140	139	137	136	136	131
95	99	106	110	114	117	131	146	140	138	136	135	132	135	128	126
93	96	100	109	112	107	130	134	138	137	129	120	121	125	125	116
95	99	109	113	118	131	131	120	120	120	114	113	140	140	135	128
97	107	128	125	135	148	128	129	130	122	121	137	163	162	147	134
113	126	132	132	141	142	151	162	162	158	155	167	169	158	143	127
110	118	123	125	131	140	166	160	170	184	170	158	147	146	131	120
104	107	119	118	132	147	165	164	161	168	156	149	148	136	130	129
100	106	126	130	145	152	148	160	148	140	142	154	140	133	123	116
113	109	120	111	130	139	150	166	166	149	140	156	155	129	105	98
114	112	125	102	118	124	154	160	160	150	142	150	139	111	100	109
104	106	121	112	130	123	152	165	147	138	126	124	115	99	110	130
109	115	136	137	151	134	166	179	146	139	128	114	111	108	117	151
114	124	158	166	186	162	183	186	158	147	137	125	124	118	123	151
125	130	161	181	189	173	176	186	171	144	126	134	126	111	108	130
132	109	148	171	178	169	158	172	169	142	120	130	130	117	109	123

Figure 6 **Computer printout of a 16 x 16 array quantifying the digital voltages of a saline solution acoutic micrograph.**

93	98	101	107	108	127	132	137	139	143	141	138	138	136	137	132
96	100	103	109	114	116	131	146	141	137	137	135	134	133	126	123
97	96	99	107	110	110	127	131	134	136	127	120	121	126	127	119
95	99	108	117	119	133	131	120	119	118	114	115	130	142	138	130
99	109	126	125	134	147	128	133	132	121	122	142	167	164	151	133
113	125	132	132	140	144	156	164	165	161	157	167	166	156	142	125
112	118	121	124	139	141	168	164	168	184	169	155	150	146	130	121
103	106	120	119	133	149	161	162	161	164	156	150	144	132	128	126
105	106	129	133	147	150	149	161	149	141	141	152	146	133	121	113
105	112	122	107	132	136	151	168	167	150	141	154	154	128	105	99
113	112	127	103	116	120	154	168	163	152	143	145	141	109	101	110
107	105	124	113	130	121	150	165	143	133	124	122	115	98	111	129
113	117	142	144	158	136	164	180	147	142	134	116	112	112	119	152
122	125	144	167	168	151	183	184	156	140	136	126	124	117	121	150
115	129	156	170	188	175	173	184	173	144	125	134	127	113	109	132
132	107	147	168	178	169	155	166	166	139	118	134	124	117	109	121

Figure 7 **The same image as that in Figure 7, but digitized five minutes later.**

where d is the difference between a pair of digital voltages and N is the number of elements in the array (N = 256 in this instance). To quantify an uncertainty value for the IL measurements, the calibration equation, Equation 11b (described later in this section) was used to define the IL value that was greatest affected by D. The IL was then recalculated to include D, and, since D can affect both Vs and Vo, the two extreme values of the ratio Vs:Vo were used, i.e., (Vs + D):(Vo - D), and (Vs - D):(Vo + D). The largest difference between the actual IL value and one of the IL values containing D is the maximum uncertainty which, in this case, is $\pm$ 2.64 dB.

The alteration of the signal was found to be random, as shown by the Gaussian distribution of the signal in Figure 8. Therefore, averaging a larger number of points increases the precision of the voltage measurements. The array size was changed from a 16 x 16 to an 8 x 8 so that each element contained 11,520 data points (60 lines by 192 points), a four-fold increase in the number of data points being averaged for each voltage value. Figures 9 and 10 illustrate 8 x 8 arrays of the same image averaged at two different times where the calculated deviation is 1.038, an improvement of greater than 50% from that of the 16 x 16 array. Each IL value, therefore, has a calculated maximum uncertainty of $\pm$ 1.15 dB. The 8 x 8 array has an improved uncertainty over the 16 x 16 array, as well as over the former technique, and was, thus, utilized as part of the new technique.

In order to know the position of an object on the microscope stage relative to the array element location on the T.V. monitor,

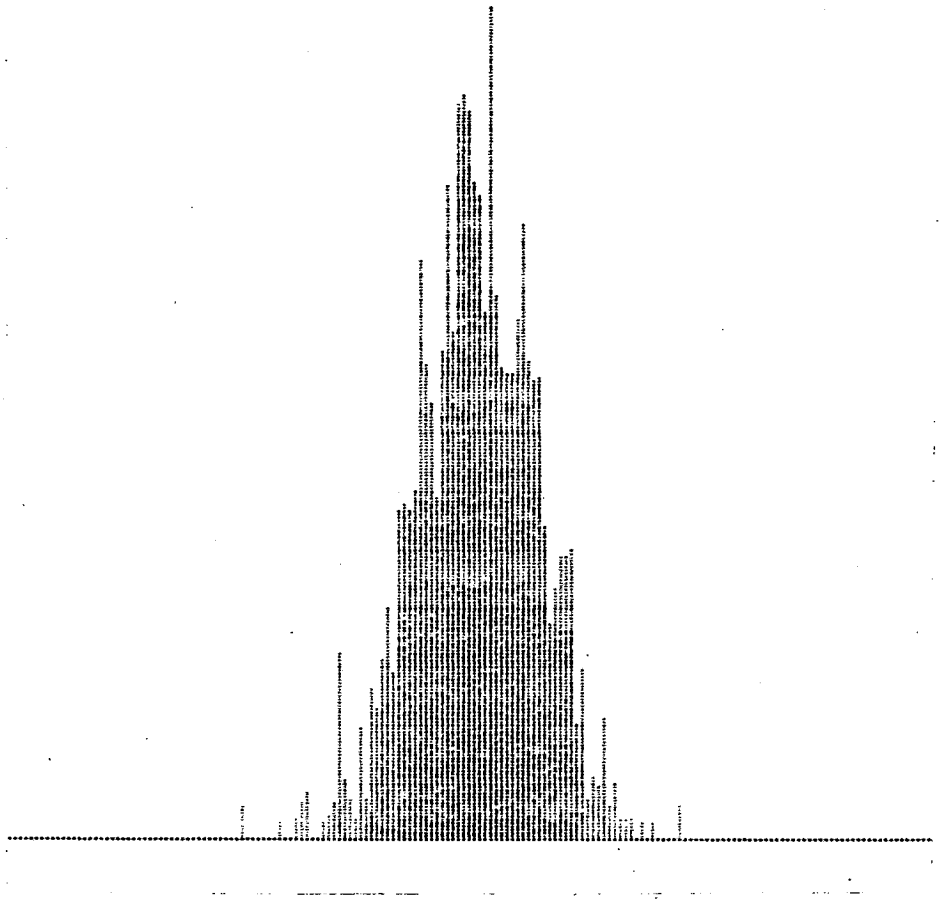

Figure 8 Computer printout of the relative signal amplitude of a single point in the acoustic image taken over a 30 second time period.

122	143	140	135	137	130	118	110
119	136	127	126	140	124	113	113
141	143	138	158	167	141	132	118
126	148	167	163	159	144	136	124
127	149	151	161	147	133	133	119
121	150	149	153	118	122	128	114
122	146	136	127	119	148	139	114
127	144	130	129	117	138	124	110

Figure 9 Computer printout of an 8 x 8 array of the average digital voltages of a saline solution image.

121	143	141	136	138	132	118	111
118	137	128	126	140	125	113	113
142	143	138	159	166	141	131	118
127	147	165	160	157	143	136	124
127	148	150	160	145	132	133	119
121	150	147	152	118	123	129	114
122	145	135	128	119	148	141	114
128	144	130	129	117	139	126	111

Figure 10 Same image as that in Figure 9, but digitized five minutes later.

the following procedure was followed. A clear plastic overlay, blocked off into 64 equal sized squares (8 x 8), was placed on the T.V. monitor. Saline was placed on the stage and a small air bubble introduced between the stage and the coverslip. The coverslip was moved around until the bubble, as viewed on the T.V. monitor, was lying solely within a single element. The image was digitized with and without the bubble and the two arrays were compared. Since air is acoustically opaque, the voltage level in the element containing the bubble was markedly lower than its pair voltage in the array without the bubble. With the exception of the one element containing the bubble the two arrays were within the deviation calculated for the 8 x 8 arrays, and the overlay was assumed correct.

To further improve the system, faster and easier access to the voltage values were needed. Approximately 5 minutes were required for the image to be digitized, averaged and printed. Since the average voltage of only a single array element was needed to find an IL value it was not necessary to digitize the entire image. Therefore, an additional program was written (see Appendix) so that only a selected element was digitized and averaged; this reduced the processing time to about 8 seconds.

If an attempt is made to substitute the digital voltage values in for Vs and Vo in Equation 3, two problems exist. First, when voltages are converted from decimal to binary the equation to find IL can no longer be used directly. To illustrate this point, consider an example where, in decimal, Vs = 500 mV and Vo = 250 mV. The ratio of Vs to Vo is then equal to 2.0. When

these voltages are converted into binary numbers, Vs = 0 and Vo = 64, yielding a ratio of zero. Second, the value of the reference voltage is unknown. These two problems were solved simultaneously. By inserting known values of electrical attenuation between the 100 MHz signal source and the ultrasonic transducers, and determining the average voltage of a certain array element as a function of the inserted electrical attenuation, a calibration curve and equation was determined.

Before the calibration equation was formed the attenuators were checked for linearity. Various thicknesses of distilled water were placed on the stage, the voltage measured, and electrical attenuation dialed in until a predetermined voltage was reached. The value read off the attenuators and the thickness of the sample were recorded and a plot was made of electrical attenuation versus thickness. The slope of the line through the points should be the attenuation coefficient of distilled water which is 135 dB/mm at 100 MHz. The plot resulted in two different slopes - that of the attenuation coefficient of water for electrical attenuation values greater than 6 dB, and a slope of 5 dB/mm for electrical attenuation values less than 6 dB. The attenuators did not provide a linear response between 0 dB and 6 dB. One explanation for this is that they are not perfectly impedance matched between the oscillator and the transducer, i.e., there is 50 kΩ ouput impedance of the oscillator, and an unknown input impedance at the transducer. Thus, a 1 dB increase in the attenuators, say from 2 dB to 3 dB, is seen by the transducer as a larger than 1 dB increase. However, the same increment, say

from 9 dB to 10 dB, is seen by the transducer as exactly a 1 dB insertion loss.

To obtain the calibration curve an image of pure saline was used, a starting electrical attenuation of 7 dB was inserted and the receiver gain was turned up so as to use the full range of the A/D. The stage was mechanically adjusted to place the brightest portion of the field near the center; one of the center array elements was then chosen and used throughout. The element was digitized, averaged and the voltage recorded. The attenuation was increased by 1 dB and the same element was, again, digitized and averaged. The process was continued until there appeared to be negligible changes in the average voltage with an increase in the electrical attenuation (about 21 dB as read off of the attenuators). The points were plotted as attenuation versus average digital voltage. To assure reproducibility of the numbers, the entire procedure was repeated four additional times and is illustrated in Figure 11 where the deviation, if one exists, is indicated by a horizontal line through the average value. Since the data closely compared, all of the values resulting from the data were used to derive a single calibration equation. The derivation is as follows. Since power, P, is proportional to the square of the signal voltage, Vs,

$$P = k(Vs^{**}2) \tag{5}$$

where k is the proportionality constant. In this case there is an unknown offset voltage, Vo, present which alters the equation to read

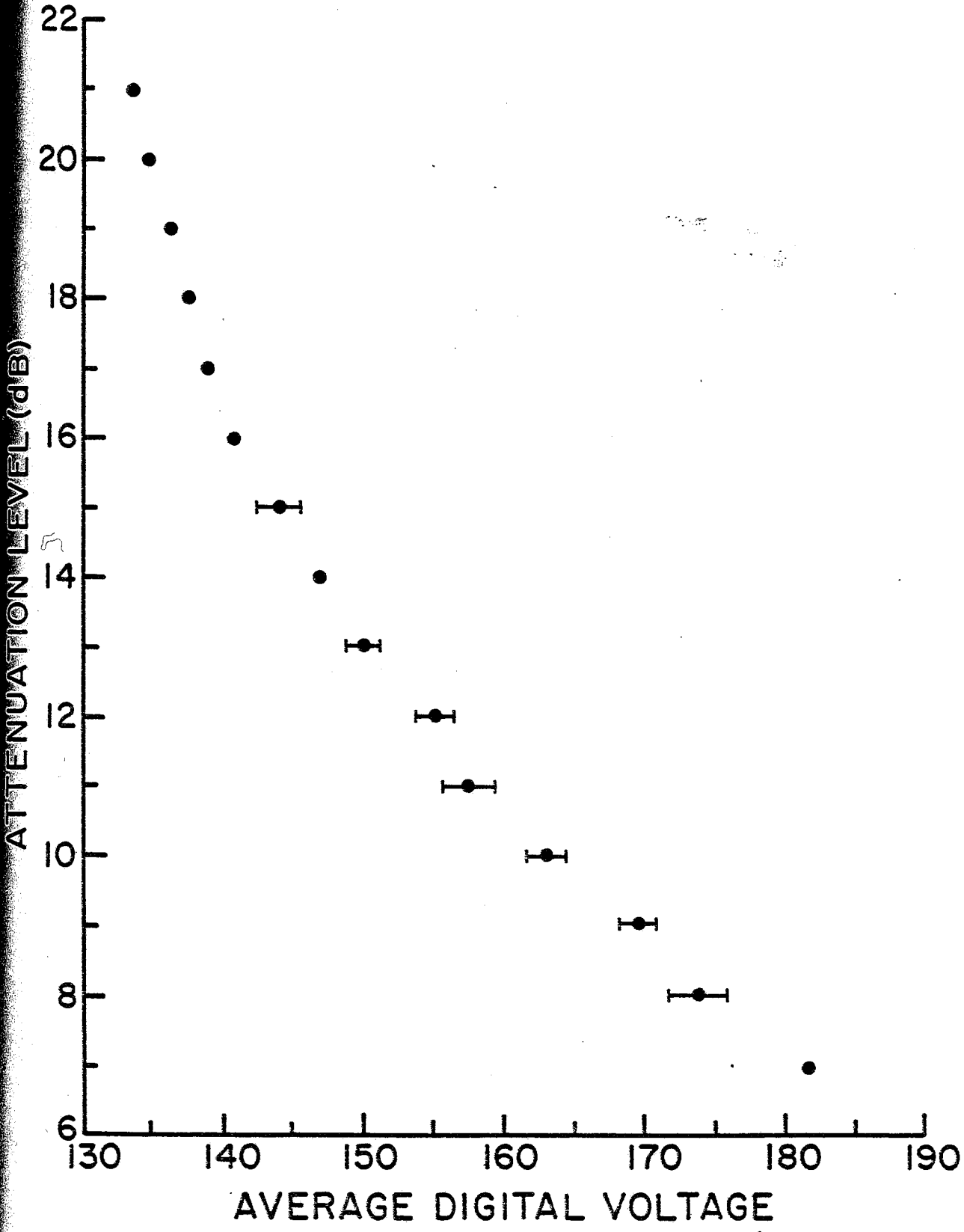

Figure 11 Calibration curve.

$$P = k[(Vs - Vo)**2]. \quad (6)$$

An operator, $-10*\log P = L$, where L has units of dB, is used to convert Equation 6 into the following form

$$10^{-L/10} = k[(Vs - Vo)**2]. \quad (7)$$

Rearrangement of Equation 7 produces

$$Vs = \sqrt{1/k}\ 10^{-L/20} + Vo \quad (8)$$

which is also the equation of the of the calibration curve. A least square fit program is used to calculate the slope ($\sqrt{1/k}$) and the intercept (Vo) with $10^{-L/20}$ being entered for the x-coordinate and Vs for y. Solving for L yields

$$L = -20*\log\left(\frac{Vs-Vo}{\sqrt{1/k}}\right). \quad (9)$$

Since it is known that

$$IL = L_2 - L_1 \quad (10)$$

where L_1 is the power in dB of the background and L_2 is the power in dB of the tissue, an equation for IL is derived

$$IL = -20*\log\left(\frac{Vs_2 - Vo}{1/k}\right) + 20*\log\left(\frac{Vs_1 - Vo}{1/k}\right) \quad (11a)$$

$$= -20*\log\left(\frac{Vs_2 - Vo}{Vs_1 - Vo}\right) \quad (11b)$$

where Vs_1 is the voltage of the signal without the tissue, i.e., the reference voltage, and Vs_2 is the voltage with the tissue in place. A digital voltage of Vo = 120.45 and a slope of 135.15 was calculated, with a resulting correlation coefficient of 0.998. The correlation coefficient refers to how well the line fits through the plotted values; the range is from 0 to 1, with 1 being the best possible fit. The final form of the calibration equation is

$$IL = -20*\log\left(\frac{Vs_2 - 120.45}{Vs_1 - 120.45}\right). \qquad (12)$$

An optimal Vs was calculated using Equation 8 and P = 7 dB. This value turned out to be Vs_1 = 180.8. When performing IL measurements, the attenuators must be set at 7 dB and the receiver gain adjusted so that the digital voltage of the background in the chosen array element is around 180.8. Vs_1 can be 180.8 $\pm$ 6 and still have less than $\pm$ 1 dB error.

A minimum Vs_2 was determined by finding the voltage value of a very attenuating specimen, i.e., an air bubble. This value turned out to be 130. The dynamic range of the system, caluculated by substituting Vs_1 = 180.8 and Vs_2 = 130 into Equation 12, is 16 dB.

CHAPTER 3

METHODS OF PROCEDURE

3.1 SPECIMEN PREPARATION

Male rats of a Spague-Dawley strain were used for this experiment. There was collaboration with the Department of Food Science to obtain the rat liver samples. They provided a sample about 1/9 the size of the liver from each rat, as well as the percentage fat assay information for each specimen. Due to the nature of the study in Food Science, the rats were broken up into four groups and fed different diets. Two groups were fed alcohol in their diets while the other two were not; two groups were fed diets that were depleted in Vitamin A, or 1/6 the Recommended Dietary Allowance (RDA) of the vitamin while the others were fed at the RDA.

The rats were fed the same basic diet with a change in either the alcohol or Vitamin A content. Due to the rats' natural aversion for alcohol, totally liquid diets were used in all four groups. The basic diet components are shown in Table 1.

The diet ingredients were added to water so that the final composition was 70% water by volume. Vitamin A as retinyl acetate (Sigma Chemical Co., St. Louis, MO) was supplemented to the diet at 1/6 the RDA or at the RDA level. In the alcohol groups absolute ethanol was isocalorically substituted for 30% of the sucrose. To keep the diet components suspended, Suspending Agent K (BioServ Inc., Frenchtown, NJ) was added at 0.5% of the water content.

TABLE 1

BASIC DIET COMPONENTS

COMPONENT	% OF VOLUME	% OF CALORIES
Casein (Vitamin-Free test casein, Tekland Test Diets, Madison, WI)	20	19.1
Fat (Corn Oil)	8	16.8
Mineral Mix (Mineral Mix V.S.P. XVII, Tekland Test Diets)	4	—
Sucrose	67	64.1
	100	100.0

After four weeks, half of the animals from each group were sacrificed, their livers removed, and a small portion cut off of each for this experiment. The pieces were quick-frozen (to prevent bursting of cells) in a dry ice and acetone solution and stored at -70°C until ready to examine. The remaining rats went through the same procedure four weeks later.

When a liver sample was ready to be examined under the microscope, a small chunk (about 0.5 cm^2 x 0.75 cm thick) was cut out of the frozen section of liver, making sure to avoid obvious inhomogeneities such as venule or arterial clusters, and sliced into four sections, as listed in Section 2.1, using the microtome. To utilize the microtome the tissue was mounted on a metal chuck using Tissue-Tek II, an O.C.T. Compound embedding medium for frozen tissue specimens. This embedding compound freezes at -30°C, dissolves in saline at room temperature, and does not appear to react with the tissue. After a single section had been defrosted and rinsed off with saline, it was trimmed with a razor blade into a triangular piece about 2 mm on each side since the microscope's field of view was 2 mm x 3 mm.

3.2 MICROSCOPE PREPARATION

The microscope stage module is pulled forward and a small amount of distilled water (about 5 drops) is placed directly on the sonically activated fused silica portion of the stage (2.5 cm x 5.1 cm). The water acts as an acoustic coupler between the stage and the plastic slide that will contain the tissue and is important to assure insonification of the sample.

The slide consists of a plastic frame with a 5 cm diameter hole cut out of the middle. A 0.50 cm thick, 0.25 cm wide metal ring fits snugly inside so that a very thin sheet of plastic (22 μm) can be mounted on the slide by wedging it in between the plastic frame and the metal ring. The thin plastic needs to be as dirt and scratch free as possible to avoid undesired alterations in the sound field and is, therefore, changed after 7-10 slices have been examined. The slide is then carefully placed on the stage making sure to avoid air bubbles. Masking tape is used between the slide frame and the periphery of the stage to secure the structure and maintain continuity.

One of the small, triangular pieces of liver is placed in a few drops of normal saline solution on the plastic slide. Saline is used as the acoustic coupling here at the slide-specimen interface.

A partially mirrored coverslip is placed on top of the biological specimen and supported by a metal washer that is larger in thickness than the thickes sample used. The spacer is used for two reasons: 1) to keep a uniform distance between the stage-slide interface and the coverslip at all times, and 2) to prevent the coverslip from compressing or distorting the tissue. The coverslip, which contains a thin gold coating on the side which will face the tissue, is used only with optically non-reflective samples, as in the case of biological media. The gold coating, if scratched, produces undesirable results in the acoustic image and, therefore, must be handled with extreme care and replaced every so often. Saline is used as a coupler at this

interface as well, and is just as important as the coupling between the stage-slide interface and the slide-sample interface.

During these experiments it was discovered that there were nonuniformities within a single coverslip, as a slight change in position of the coverslip would result in an alteration of the signal. For this reason two pieces of masking tape were placed at right angles to each other in the upper left-hand corner of the slide so that the coverslip could be abutted against it and thus be repeatedly positioned.

The stage is positioned so that the specimen is located in the field of view. Initial focusing of the image is done while viewing the optical mode of the microscope by moving the stage up or down until a clear image appears. Further adjustments take place in the acoustic mode using two micrometer controls that angle the stage in mutually perpendicular directions (yaw and pitch). Since rotation of one or both of these micrometers change the area of tissue exposed to the laser, a desirable setting occurs at an optimum image signal level and field uniformity.

3.3 DATA COLLECTION

For each liver sample, four thicknesses of tissue were analyzed in order to determine an attenuation coefficient. The time it takes to collect the data for one sample ranges between two and four hours.

Data for an insertion loss measurement are taken from two different locations in each section for a total of eight IL values from each liver sample. An element on the screen is chosen from

the 8 x 8 array, usually close to the center and in the brightest, most uniform spot. An initial digital voltage of about 180 must be achieved without the tissue in place, as described in Section 2.2. The receiver gain is then adjusted to achieve a desirable starting average digital voltage for that element, and this number is recorded as Vs_1. The stage is carefully pulled forward, the coverslip lifted, and the tissue repositioned so that it will lie in the chosen element area. The coverslip is replaced and the stage pushed back into the microscope. Often, the steps to position the tissue must be repeated many times for two reasons: 1) to maneuver the tissue so that it completely covers the element because the tissue has a tendency to move when the coverslip is laid down, and 2) to eliminate any air bubbles. With the tissue in place another voltage measurement is taken. A slight adjustment in focusing the acoustic image may be necessary again, so the two micrometers that yaw and pitch the stage are fine tuned for a maximum voltage, and the voltage then recorded.

To obtain the second set of data for this thickness, the tissue section is moved out of the chosen element and another voltage taken. A voltage of 180 should be obtainable by simply fine tuning the micrometers and not adjusting the gain or moving to a new area of the sound field. The tissue is then inserted so that a different region lies in the the array element. Again, the stage is fine tuned for a maximum voltage.

Using the same tissue section the velocity data is also collected. The microscope is switched from the acoustic to the interference mode of operation where the acoustic phase can be

measured as the wave propagates through the saline and the tissue. The tissue must again be repositioned, this time so that some of the interference lines travel through the saline into the tissue and back out into the saline.

Once the tissue is in place the receiver gain must be decreased so that the signal lies within the range of the A/D. The program is then cued to exit the voltage calculation section and begin the digitization of the image. During this time the microscope stage must not be jarred, nor any of the knobs adjusted. When the image is digitized and has been stored on tape, the correlation program will begin. During the correlation the tissue can be removed and a new setup prepared. It is a good idea to rinse off the coverslip, as well as replace the saline in the slide, before introducing a new slice of tissue. This is the time to replace the coverslip or the thin plastic of the slide if a flaw exists in either structure. After a maximum of ten thickness measurements have been made using the same plastic, or at the end of a days work, the plastic is changed regardless. The entire procedure is repeated for the other sections.

CHAPTER 4

TECHNIQUE VERIFICATION

To verify the new technique, aqueous solutions of Bovine Serum Albumin (BSA) Fraction V were chosen because of the availability of attenuation data at 100 MHz (Kessler and Dunn, 1969). The data are presented in terms of the excess frequency-free absorption per unit concentration

$$A = \Delta a/cf^2 \tag{13}$$

where c is the concentration of the solution in grams per cubic centimeter, f is the frequency, and Δa is the difference between the attenuation coefficient of the solution (α_{SOL}) and the attenuation coefficient of the water (α_{H_2O}),

$$\Delta a = \alpha_{SOL} - \alpha_{H_2O} . \tag{14}$$

The attenuation coefficient of the BSA solution is

$$\alpha_{BSA} = Acf + \alpha_{H_2O} . \tag{15}$$

At f = 100 MHz, A = 30×10^{-16} $s^2 \cdot Np \cdot cm^{-1} \cdot cc \cdot gm^{-1}$ (Kessler and Dunn, 1969). Furthermore, α_{H_2O} = 2.5 Np/cm. Equation 15 then becomes

$$\alpha_{BSA} = c(30\ Np \cdot cm^{-1} \cdot cc \cdot gm^{-1}) + 2.5\ Np \cdot cm^{-1} . \tag{16}$$

Two concentrations of BSA solution were made up by dissolving known amounts of BSA powder into distilled water and precisely measuring the final volumes. The concentrations used were 0.0347 gm/cc and 0.0935 gm/cc which, from Equation 17, yield

attenuation coefficients of 3.54 Np/cm (30.76 dB/cm) and 5.31 Np/cm (46.08 dB/cm), respectively.

The IL of these two specimens were measured at several thicknesses using the same basic procedure as described in Sections 3.2 and 3.3. The major difference was that since the specimen was a liquid, various spacer thicknesses were used to obtain a range of sample thicknesses. Also, Vs was adjusted before the slide was filled with BSA solution by measuring the digital voltage of a very thin layer of distilled water (about 1 drop). For the 3.47% BSA solution the IL was found at four thicknesses; 0.1672 cm, 0.2045 cm, 0.3252 cm, and 0.4745 cm. The 9.35% solution utilized three thicknesses because the expected IL at 0.4745 cm would have been larger than the dynamic range of the measurement technique.

Two IL values were found at each thickness. The ultrasonic attenuation coefficients of BSA solution at 100 MHz for each solution were calculated to be: 29.86 dB/cm for c = 3.47% and 45.70 dB/cm for c = 9.35%. The values compare to the published results to within 2.9% and 0.8%, respectively.

CHAPTER 5

RESULTS AND DISCUSSION

One of the purposes of this investigation was to develop semi-automated methods for data collection of attenuation and velocity measurements and this task was successfully completed. The SLAM was interfaced to a computer through a data acquisition system and programs were written to process the data. The programs were accessible through a remote computer terminal at the microscope room which permitted the operator to remain at the microscope.

The technique to determine velocity utilizes the DAS to digitize the interference image so that fringe shift values, N, can be found. The resulting hard copies have much better resolution, in most cases, than the photographs of the former method. Because of the increase in resolution of the fringe lines, the determinations of N are made with greater accuracy.

Some of the digitized interference patterns had fringed lines that were very undefined. This was traced, not to the DAS, but to the noisy images from the microscope itself. These poor quality images were usually observed after the microscope had been in operation for at least six hours and were accompanied by a decrease in the laser power level of the microscope.

On other hard copies of the interference pattern the length of the shift would drastically increase from the center to the edge of the image. It was determined that when the image was too close to the left or right edge of the sound field, the

interference lines would bow outward, thus, causing the shifts through the tissue to appear larger than they should have been. This problem can be eliminated by carefully monitoring the interference image, as seen on the T.V. monitor, before cueing the program.

The technique developed to measure insertion losses also uses the DAS, but only digitizes one portion (element) of the image so that an average voltage can be found and displayed on the computer terminal. This method is more objective than the one formerly used.

There was often a problem measuring IL due to the noisy signal, as was just mentioned in the case of the poor interference images. Two other, usually joint problems, were the insertion of the specimen into the correct array element and elimination of air bubbles from the field of view. These were often very time consuming steps, and, if it took too long, the tissue (especially the thinner sections) tended to fall apart. The consequences were a thinner specimen and a "sea" of floating debris surrounding the specimen.

Another purpose of this study was to investigate the elastic properties of rat livers of varying fat content using the SLAM. Collaboration with the Department of Food Science occurred because one of their research groups was studying the effects of alcohol intake on rat livers, claiming that prolonged alcohol, in conjunction with a nutritionally adequate diet can produce a fatty liver. They were also interested in the effects of Vitamin A on the liver, hence, the four different diets (Section 3.1). By

determining the ultrasonic attenuation coefficient and velocity of the livers, it was hoped that a correlation between these quantities and fat content be discovered. If, indeed, there were measurable effects due to increasing fat content, namely, increasing attenuation coefficients and decreasing velocity values, the results could be useful in the early detection and possibly the clinical treatment of fatty liver disease.

Twenty-nine liver samples were measured and analyzed for attenuation coefficients and acoustic velocity. Four of the rats were fed normal diets, i.e., Vitamin A at the RDA level and no alcohol, and are considered shams in this investigation. Table 2 summarizes the fat content, velocity, and attenuation coefficient, as well as the correlation coefficient of the last parameter, for each sample.

After the collection of the data it was discovered that none of the livers achieved a "fatty" stage. The fat content range of these samples is 2.6-5.1 % lipid/gm wet-wt liver and a liver is not considered "fatty" until a minimum value of 9% is achieved. As a result, the data clustered in the "normal" and slightly above normal fat concentration.

Figure 12 represents the distribution of the attenuation coefficients as a function of fat content in the liver, and, even though none of the livers are considered "fatty", the data suggests a possible increase in the attenuation coefficients with increasing fat content. The average attenuation coefficient is 15.4 ± 3.7 dB/mm. Recent compilations (Goss et al., 1980) have shown that there is no data base of rat liver attenuation

TABLE 2

ULTRASONIC PROPAGATION PROPERTIES OF RAT LIVER SPECIMENS

% LIPID	ATTENUATION COEFFICIENT (dB/mm)	CORRELATION COEFFICIENT	VELOCITY (m/s) Cx(max)	Cx(min)	
2.61	14.2	.87	1570	1524	
2.86	10.5	.66	1587	1528	
2.94 *	15.7	.87	1589	1522	1555.5
3.13	19.7	.84	1586	1545	
3.16 *	8.1	.70	1560	1545	1552.5
3.19 *	18.4	.93	1588	1542	1565.0
3.20	14.0	.75	1584	1529	
3.21	11.4	.70	1593	1534	
3.25	15.8	.93	1595	1534	
3.37	19.1	.95	1563	1529	
3.40	14.8	.76	1578	1538	
3.41	14.2	.87	1587	1536	
3.41	18.0	.74	1576	1531	
3.46	20.7	.89	1588	1534	
3.62 *	8.4	.55	1575	1533	1554
3.76	15.5	.84	1569	1540	
3.77	15.9	.86	1578	1529	
3.85	23.9	.96	1595	1557	
3.87	18.2	.94	1556	1531	
4.00	9.9	.84	1589	1524	
4.02	16.9	.66	1570	1532	
4.03	12.1	.91	1539	1524	
4.04	16.1	.63	1584	1529	
4.09	17.1	.90	1577	1531	
4.38	11.6	.97	1580	1544	
4.41	13.6	.75	1569	1525	
4.84	21.5	.99	1600	1525	
4.91	16.1	.90	1563	1530	
5.08	15.8	.82	1589	1537	

* SHAMS

29 K Hashem

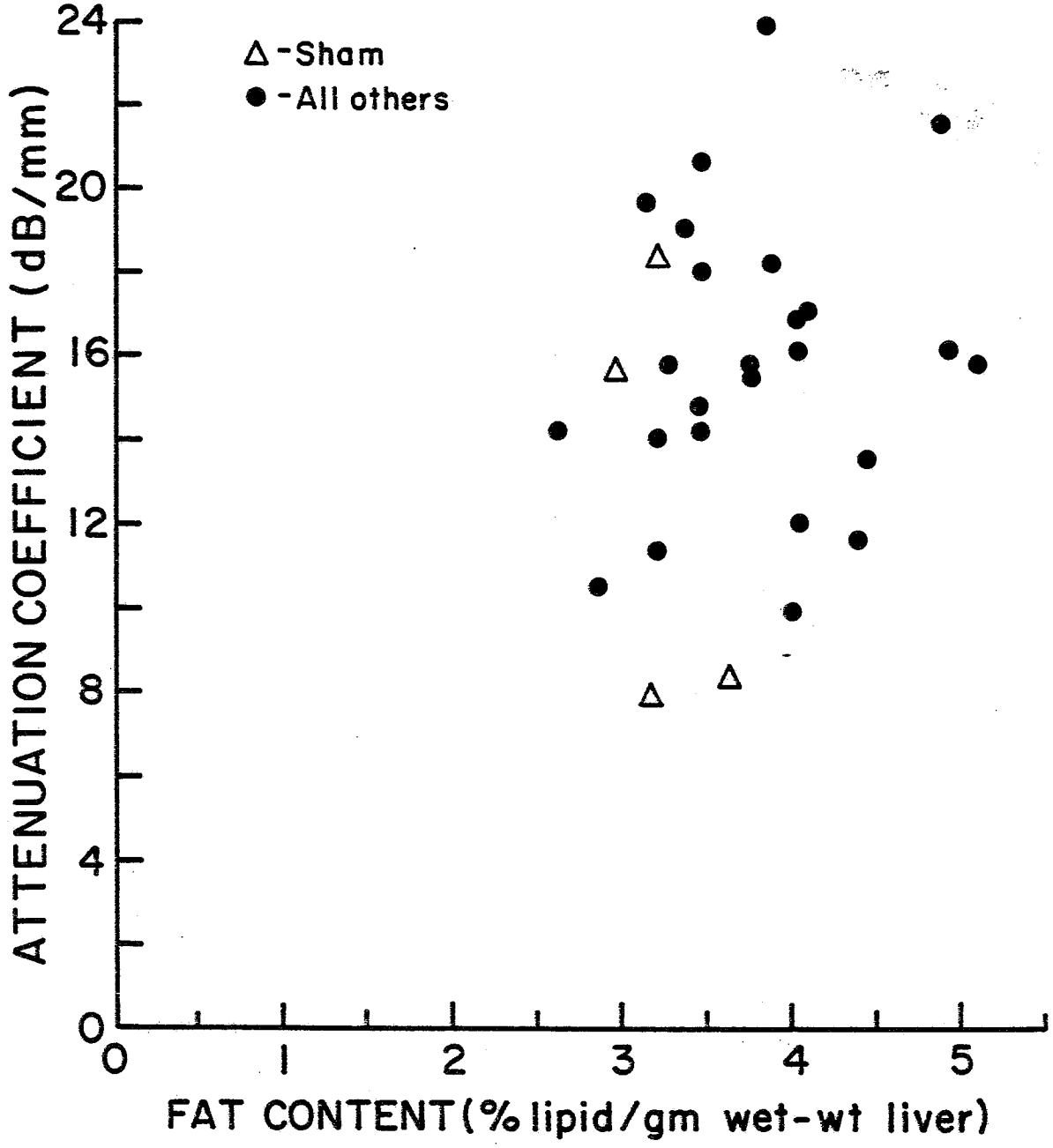

Figure 12 Distribution of attenuation coefficients versus fat content.

coefficients as a means of comparison. However, attenuation coefficients at 100 MHz of fresh bovine liver, 13.4 $\pm$ 1.7 dB/mm (Pohlhammer et al., 1981), can be compared to the current results due to the fact that 1) the organs serve the same metabolic function in both animals, and, 2) the fat content in beef liver, 3.8% (Watt and Merrill, 1963), lies within the range of rat liver fat content obtained in this study. The discrepancy between the attenuation coefficients of the two species may be attributed to the difference in preparation of the specimens, i.e., fresh versus fast-frozen.

The desired end-result of this study was a range of Cx (Equation 1) values rather than an average value for each liver sample. The three reasons for this decision are as follows: 1) There is currently no velocity data for rat liver (Goss et al., 1978), 2) there is limited velocity data for any organ at 100 MHz, and 3) the velocity may not even remain constant throughout any tissue, regardless of its homogeneity. Figure 13 shows the range of velocity measurements at various levels of fat content. It can be seen that the velocity range remains fairly constant, despite a slight increase in fat content. Fresh beef liver, measured at lower frequencies yields average velocities in the range 1545-1641 m/s (Goss et al., 1980), and can also be compared to the current data because reports show that little difference exists in ultrasonic velocity measured at various frequencies in the 1-100 MHz range (Goss et al., 1978).

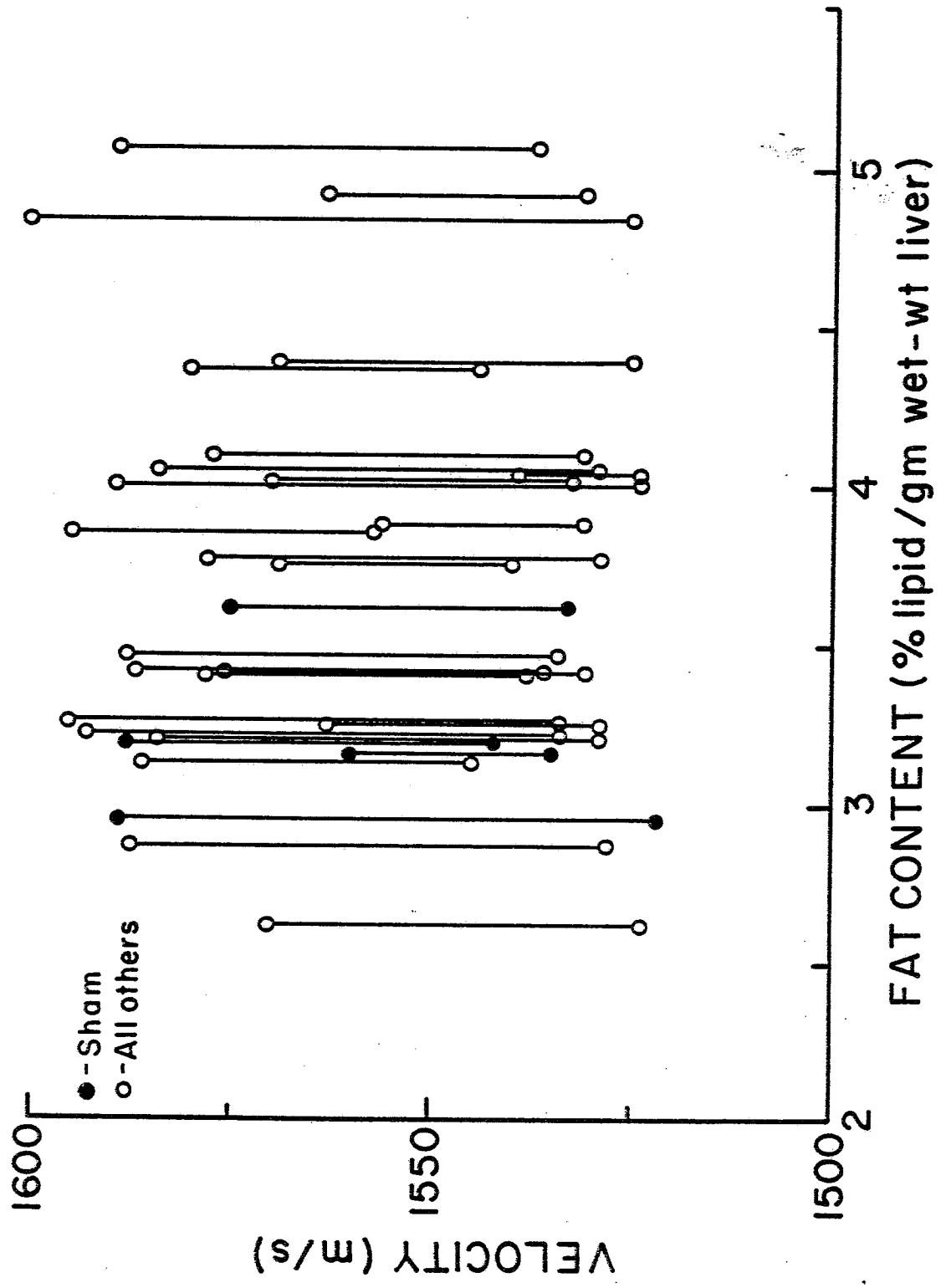

Figure 13 Velocity range versus fat content.

CHAPTER 6

IMPROVEMENTS

Three problems intrinsic to the SLAM must be dealt with by the manufacturer: 1) the signal drift, 2) the sound field nonuniformity, and 3) the laser power level drop off. The drift leads to a randomness of the voltage averages and the interference lines, thus, affecting both attenuation and velocity measurements. The nonuniform field opens up more room for error in the attenuation measurements. The decrease in the laser power creates a "noisier" picture and introduces error into both sets of measurements. Improvements to the SLAM in these three areas would greatly enhance the image quality as well as increase the credibility of the measurement techniques.

The velocity measurement technique could be improved by decreasing the digitization time of the image through either bettering the existing program or increasing the buffer memory. Further enhancement could be provided by fully automating the system through additional software so that the fringe shift values and velocities be determined by the computer.

The attenuation measurement technique could also be fully automated through some additional programming and circuitry. A program could be written to contain the equations of IL and the attenuation coefficients, as well as commands to adjust the receiver gain to a predetermined level from signals provided through an external feedback loop. The operator would then only have to arrange the slide, specimen and coverslip to an

appropriate starting postion on the stage and the computer would take over from there. This technique could also be improved by plotting another calibration curve that had a starting digital voltage closer to 255 (it was around 180 in this case). This would increase the dynamic range of the measurement system from 16 to 25 dB. An improvement in the uniformity of the coverslips would also enhance this measurement technique. In this manner the tissue could be placed on one side of the image with saline on the other side and the setup left untouched through the data collection. Voltage averages could then be made in two different array elements (where the sound field is uniform) - one from an area of pure saline and one from that of just tissue.

REFERENCES

Foster, S. (1981). An Image Digitizing System for a Scanning Laser Acoustic Microscope, M.S. Thesis, University of Illinois at Urbana-Champaign.

Goss, S.A., Johnston, R.L. and Dunn, F. (1978). Comprehensive Compilation of Empirical Ultrasonic Properties of Mammalian Tissues. J. Acoust. Soc. Am. 64, 423-457.

Goss, S.A. and O'Brien, W.D., Jr. (1979). Direct Ultrasonic Velocity Measurements of Mammalian Collagen Threads. J. Acoust. Soc. Am. 65, 507-511.

Goss, S.A., Johnston, R.L. and Dunn, F. (1980). Compilation of Empirical Ultrasonic Properties of Mammalian Tissues.II. J. Acoust. Soc. Am. 68, 93-108.

Kessler, L.W. and Dunn, F. (1969). Ultrasonic Investigation of the Conformal Changes of Bovine Serum Albumin in Aqueous Solution. J. of Physical Chemistry, 73, 4256-4263.

Kessler, L.W. (1973). High Resolution Visualization of Tissue With Acoustic Microscopy. Ultrasonics in Medicine, Proceedings of the 2nd World Congress on Ultrasonics in Medicine, Rotterdam, The Netherlands, 4-8 June 1973. Edited by M. de Vlieger, D.N. White and V.R. McReady. Excerpta Medica, Amsterdam., 249-256.

Lieber, C.S., Jones, D.P. and DeCarli, L.M. (1965). Effects of Prolonged Ethanol Intake: Production of Fatty Liver Despite Adequate Diets. J. Clinical Investigations, 44, 1009-1021.

Pohlhammer, J.D., Edwards, C.A. and O'Brien, W.D., Jr. (1981). Phase Insensitive Ultrasonic Attenuation Coefficient Determination of Fresh Bovine Liver Over an Extended Frequency Range. Medical Physics, (In Press).

Watt, B.R. and Merrill, A.L. (1963). Composition of Foods. Agriculture Handbook No. 8, U.S. Department of Agriculture, Superintendent of Documents, U.S. Government Printing Office, Washington, D.C.

APPENDIX

```
      INTEGER*4 RGSTR(16),PIXEL
      INTEGER*2 AVER,DELAY,LINE1,LINE2
10    CONTINUE
      WRITE(1,1)
1     FORMAT(' ENTER PIXEL COORINATE (I1,I1)  ')
      READ(1,2)I1,J1
2     FORMAT(2I1)
      IF(I1.EQ.0) GOTO 6
      IF(I1.EQ.9) STOP
      IF(J1.EQ.9) STOP
      I=I1
      J=J1
6     CONTINUE
      LINE1=60*(I-1)+2
      LINE2=LINE1+59
      DELAY=89*(J-1)+1172
      AVER=4
$ASSM
DIOOUT   EQU   0
DIOIN    EQU   1
TEMP1    EQU   2
FLAG     EQU   3
LINE     EQU   4
TEMP2    EQU   10
CNTR1    EQU   11
PIX1     EQU   13
AVECT    EQU   14
         STM   0,RGSTR
         LHI   DIOOUT,X'00A8'
         LHI   DIOIN,X'00A9'
         LHI   TEMP1,X'00C0'
         OCR   DIOOUT,TEMP1
         OCR   DIOIN,TEMP1
         LI    TEMP1,Y'00010000'
         SH    TEMP1,DELAY
         EXBR  TEMP2,TEMP1
         NHI   TEMP2,X'00FF'
         OHI   TEMP2,X'F100'
         WHR   DIOOUT,TEMP2
         NHI   TEMP1,X'00FF'
         OHI   TEMP1,X'F300'
         WHR   DIOOUT,TEMP1
         LHI   TEMP1,X'F907'
         WHR   DIOOUT,TEMP1
         LIS   FLAG,0
         LIS   PIX1,0
         RHR   DIOIN,TEMP1
         LH    AVECT,AVER
NEWPIX   LH    LINE,LINE1
```

```
          LIS    LINE+1,1
          LH     LINE+2,LINE2
LINLOOP   LHI    TEMP1,X'FF39'
          WHR    DIOOUT,TEMP1
BUSY      SSR    DIOIN,TEMP1
          BTBS   8,BUSY
          LHI    TEMP1,X'06E6'
          LR     TEMP2,LINE
          SRLS   TEMP2,1
          BNCS   JUMP1
          AHI    TEMP1,X'0106'
JUMP1     SR     TEMP1,TEMP2
          EXBR   TEMP2,TEMP1
          NHI    TEMP2,X'00FF'
          OHI    TEMP2,X'FB00'
          WHR    DIOOUT,TEMP2
          NHI    TEMP1,X'00FF'
          OHI    TEMP1,X'FD00'
          WHR    DIOOUT,TEMP1
          AIS    FLAG,1
          CHI    FLAG,1
          BNES   JUMP2
          RHR    DIOIN,TEMP1
          B      LINLOOP
JUMP2     LHI    CNTR1,89
LOOP2     RHR    DIOIN,TEMP1
          EXBR   TEMP2,TEMP1
          NHI    TEMP1,X'00FF'
          NHI    TEMP2,X'00FF
          AR     PIX1,TEMP1
          AR     PIX1,TEMP2
          SIS    CNTR1,1
          BNZS   LOOP2
          BXLE   LINE,LINLOOP
          SIS    AVECT,1
          BNZ    NEWPIX
          ST     PIX1,PIXEL
          LM     0,RGSTR
$FORT
      X=FLOAT(PIXEL)/FLOAT(60*178*AVER)
      WRITE(1,4)I,J,X
4     FORMAT(' PIXEL(',I1,',',I1,')=',F5.1)
      WRITE(6,4)I,J,X
      GOTO 10
      STOP
      END
```